



Hybrid carbon/glass fiber composites: Micromechanical analysis of structure–damage resistance relationships



Leon Mishnaevsky Jr.^{*}, Gaoming Dai

Department of Wind Energy, Technical University of Denmark, Roskilde, Denmark

ARTICLE INFO

Article history:

Received 31 May 2013

Received in revised form 2 August 2013

Accepted 12 August 2013

Available online 21 October 2013

Keywords:

A. Polymer–matrix composites (PMCs)

A. Hybrid composites

C. Damage mechanics

C. Modeling

ABSTRACT

A computational study of the effect of microstructure of hybrid carbon/glass fiber composites on their strength is presented. Unit cells with hundreds of randomly located and misaligned fibers of various properties and arrangements are subject to tensile and compression loading, and the evolution of fiber damages is analyzed in numerical experiments. The effects of fiber clustering, matrix properties, nanoreinforcement, load sharing rules on the strength and damage resistance of composites are studied. It was observed that hybrid composites under uniform displacement loading might have lower strength than pure composites, while the strength of hybrid composites under uniform force loading increases steadily with increasing the volume content of carbon fibers.

© 2013 Elsevier B.V. All rights reserved.

1. Introduction

Hybrid composites attract a growing interest of scientific community, among others, with view on their application as wind blade materials. While the glass fibers are relatively cheap and easily available, polymer composites with carbon fiber reinforcement show much higher stiffness, tensile strength and lower weight than those with glass fiber reinforcement. The disadvantages of carbon fibers are their high price and relative low compressive strength. So, the idea to combine these two groups of fibers to achieve the advantages of both and to reduce the weaknesses of each of them was formulated. As noted by Ong and Tsai [2], the full replacement of glass fibers by carbon fibers for a given 8 m blades would lead to 80% weight savings, and cost increase by 150%, while a partial (30%) replacement would lead to only 90% cost increase and 50% weight reduction. In a number of works, the strength and damage mechanisms of hybrid composites were studied [1–7]. It was reported, among others, that the incorporation of glass fibers in carbon fiber reinforced composites allows the improvement of their impact properties and tensile strain to failure of the carbon fibers. Apparently, hybrid composites have a great potential for the energy and structural applications.

Apart from hybrid structures, there exist several other promising directions to enhance the strength, damage resistance and lifetime of fiber reinforced composites by varying their microstructures: clustering of fibers and hierarchization of microstructures, nanoreinforcements in matrix and on the fiber/matrix

interfaces, oriented nanoreinforcements, various distributions of fibers in clusters, modifications of matrix properties [8].

The question arises – how do these modifications of microstructures influence the damage resistance of composites, alone or in combinations? Which arrangements of fibers and reinforcements, and which combinations of properties ensure the optimal service properties of the material?

In this paper, we seek to investigate numerically the effect of the microstructural modifications (like fiber mixing, clustering, nanoreinforcements and matrix modification) on the damage resistance of the composites under both tensile and compression loading. In so doing, we use statistically generated unit cells with hundreds of randomly located and misaligned fibers with various properties and arrangements. These unit cells are subject to tensile or compression loading, and the evolution of fiber damages is analyzed. Using the Weibull condition of fiber cracking and (for the special case of carbon fiber compression) Budiansky–Fleck kinking condition [9], we calculate the amount of failed fibers and analyze the microstructure–damage relationships for different materials. As a result, we seek to determine which factors and parameters can be used to enhance the composite strength and damage resistance.

2. Simple fiber bundle based model of hybrid composite

In this section, we present a simple modeling approach for the numerical testing of various microstructures of UD composites under axial loading. This includes the automatic unit cell generation code, the simplified estimation of the elastic properties of embedded fibers and the load redistribution/damage estimation methods.

^{*} Corresponding author. Tel.: +45 60697858; fax: +45 4677 5758.

E-mail address: lemi@dtu.dk (L. Mishnaevsky Jr.).

2.1. Generation of the unit cell with various fiber distributions

For the numerical analysis, a computer program “HybridFib” was developed, which generates interactively unit cells with a pre-defined amount, arrangement and properties of fibers.

Using the Monte-Carlo method, a given amount of fibers are assigned carbon or glass properties, and they are randomly arranged in the cells, using the RSA (random sequential absorption) algorithm [10–12] (i.e., the location of a fiber is calculated by random number generator, and the programs checks whether any other fibers are located too close; if yes, the next random number/location is generated, and so on), or, alternatively, clustered. Depending on this type, the radius of the fiber and its elastic and strength properties (Weibull parameters) were determined. Further, the misalignment angles are assigned to each fiber, using random normal number generator (with truncated Gaussian probability distribution, from -5° to 5°) [10,12]. The clustered arrangement of fibers was generated following the algorithm from [9,14]. First, the given amount of cluster centers was arranged randomly inside the cell, with pre-defined minimal distance between them. Then, the fibers were placed close to the cluster center, using the normally distributed parameter (distance between particle center and cluster center) and uniformly distributed angles between the line from the particle to cluster center, and the vertical. In this code, the minimal allowed distance between the cluster centers was $2.7L/m$, where L is the unit cell size and m is the total amount of clusters. The variance of the normal distribution of the distances between the particle centers and the cluster center was taken 0.0012 mm, to ensure rather close location of the particles near the cluster center [13].

Also, several more complex fibers arrangements have been designed to investigate the combined effect of fiber clustering and the mixing on the damage resistance, among them:

- (1) “Segregated” clusters: the fibers are arranged in clusters, each cluster contains either only carbon or only glass fibers.
- (2) “Mixed” clusters: in this case, we consider two cases, “outer strong/inner weak” (where carbon fibers are located on the outer border of each cluster, while glass fibers near the center of clusters) versus “inner strong/outer weak” clusters.

Fig. 1a shows an example of a “segregated” structure of the composite. Fig. 1b shows “mixed” types of microstructures: carbon fibers in the centers of clusters, glass fibers outside, and, inverse case, glass fibers inside the clusters, carbon is outside. The structures shown on these figures have 250 fibers, the amount of fibers is equal (125/125), and the total volume content of fibers is 25%.

Then, the unit cells were subject to axial loading, either tensile, compressive or repeated. For each fiber, the fiber cracking or kinking condition is checked, using the corresponding Weibull criterion (for tensile or compressive cracking) or using the Budiansky–Fleck condition for kinking [9]. The loadings were carried out in “slow” regime (i.e., after a fiber is failed, the stress on the remaining fibers increases instantly according to the “effective stress concept” and “load sharing rule”, and so on for all the fibers which fail successively one after another [9]).

2.2. Calculation of stresses on fibers

Let us consider the unit cell of N slightly inclined (in average, vertical) fibers subject to vertical displacement (strain ε). The probability of a failure (or, fraction of failed fibers) is determined using the Weibull distribution:

$$D = \text{Prob}\{\sigma \geq \sigma_{cr}\} = 1 - \exp\left[-\left(\frac{\sigma}{\sigma_{cr}}\right)^m\right], \quad (1)$$

here σ_{cr} , m – Weibull parameters. Let us estimate the stress σ in a given fiber. Following [9,15–17], we assume that the applied strain is a constant, and the stress on a given fiber is therefore a function of local elastic properties:

$$\sigma_{loc} = E_{local}\varepsilon \quad (2)$$

(as noted below, the value E_{local} is a function of the local fiber misalignment).

As a result of the load sharing (e.g., due to the fiber failure), the local stress increases by some value $\Delta\sigma$. Thus, we can write for the stress on a fiber:

$$\sigma = E_{loc}\varepsilon + \Delta\sigma, \quad (3)$$

For the case of the uniform force loading, the stress on all the fibers was assumed to be constant at the beginning, and redistributed when fibers begin to fail.

Using the three-fiber model with one broken fiber, and representing the third remaining intact fiber as a cluster of fibers, one can calculate the increase of local stress due to the load sharing $\Delta\sigma$ as [18]:

$$\Delta\sigma = \sigma_{loc} \frac{A_0 E_0}{\sum A_N E_N} F \quad (4)$$

where A_0 , E_0 , A_N , E_N – cross-sectional area and Young modulus of the broken fiber (0) and all the intact fibers (N), F – load transfer factor. For F , one can use the following formulas from as a first approximation [18]:

$$F = \frac{1}{\pi} \sin^{-1} \left(\frac{r_i}{d_i} \right) \quad (5)$$

where r_i and d_i – fiber radius and inter-fiber separation for a given i -th fiber. This approximation gives almost linear relationship between the interfiber distance and F .

Another approach to simulate the load sharing is presented in [9], and includes the power load sharing law:

$$\sigma \propto r^{-k}, \quad (6)$$

where σ is the stress on a given fiber, r the distance between a failed and the considered fiber, k the power coefficient. In our simulations, we used the power loading sharing law. Following [9], we have chosen the power coefficient -2 in the simulations. Still, the effect of the coefficient of load distribution on the damage evolution will be studied separately below.

2.3. Estimation of elastic modulus of an embedded misaligned fiber

Let us estimate the elastic modulus for a single misaligned (inclined) fiber embedded into the matrix. The embedded fiber can be presented as an inclined cylinder in a hexagon. In order to simplify the model, we transform the cell in the following way: the cylindrical fiber is replaced by an equivalent form with squared section and the same volume content in the cell. Then, the cell is divided into the vertical parts without fibers and the vertical part containing fiber as shown in [19].

The replacement of the cylindrical fiber by a fiber with squared section allows us to use the formula for Young modulus (in the vertical direction) of a laminate with inclined fiber [19]:

$$E_{elt} = \left[\sin^4 \beta / E_l + \left(\frac{1}{G_{lt}} - \frac{2\nu_{lt}}{E_l} \right) \sin^2 \beta \cos^2 \beta + \cos^4 \beta / E_t \right]^{-1} \quad (7)$$

where $E_l = E_f \nu_{Cl_{loc}} + E_m(1 - \nu_{Cl_{loc}})$; $E_t = E_f E_m / E_l$; $\nu_{lt} = \nu_f \nu_{Cl_{loc}} + \nu_m(1 - \nu_{Cl_{loc}})$; $G_{lt} = G_f G_m / [G_f \nu_{Cl_{loc}} + G_m(1 - \nu_{Cl_{loc}})]$, E_f , E_m , E_l , E_t – Young modulus of fiber, matrix, Reuss and Voigt averaged values, ν_f , ν_m , G_f , G_m – Poissons ratio and shear modulus for fiber (f) and matrix

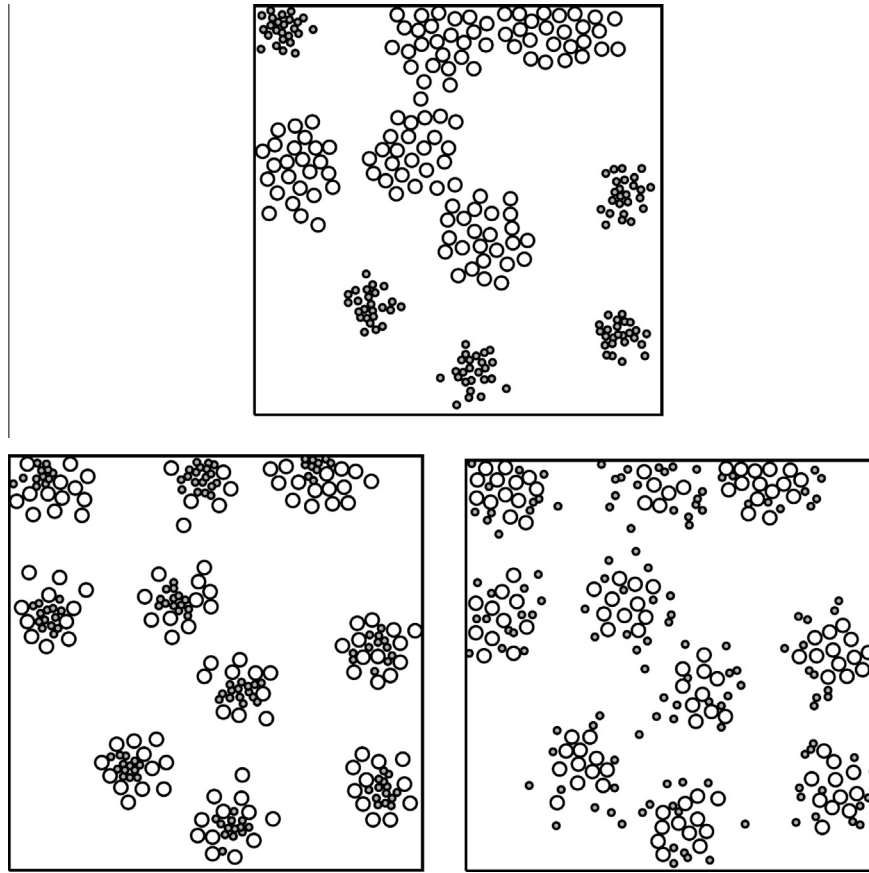


Fig. 1. Fiber arrangement in clustered hybrid composite: (a) “Segregated” microstructure, (b) mixed structure, carbon fibers in the centers of clusters, glass fibers outside, and (c) inverse case.

(m) materials, vc_{loc} – volume content of fiber material in the vertical part, containing the fiber.

Applying the rule of mixture, we can write the formula for the vertical stiffness of the composite with inclined cylindrical fiber and given volume content of fibers:

$$E_{disc} = \frac{E_{elt}ah^2 / \tan \beta + E_m(3.464hr^2 - ah^2 / \tan \beta)}{3.464hr^2} \quad (8)$$

or

$$E_{disc} = \frac{E_{elt}ah}{3.464r^2 \tan \beta} + E_m(1 - ah/3.464r^2 \tan \beta)$$

here h is the height of the unit cell, VC the volume content of fibers in the composite, and β is the angle of the fiber axis with the horizontal plane, a the linear size of the section of the equivalent quadratic fiber, $a = (vc^* v_{hex}^* \sin \beta / h)^{1/2}$, v_{hex} the volume of the hexagon (part of volume containing the fiber), $v_{hex} = 6hr^2 - tg(30^\circ) = 3.464hr^2 = [6tg(30^\circ)/\pi] v_{ic} = 1,102 v_{ic}$, r and v_{ic} the radius and the volume of inscribed circle/cylinder, h the section height. The formulas (7) and (8) give the estimation of the Young modulus of a composite (single fiber unit cell), depending on its misalignment.

2.4. Material properties

In our simulations, we use the following properties of components and materials considered:

- **Carbon fibers:** radius $r = 7 \mu\text{m}$; expected tensile strength 3000 MPa [20]; Young modulus 276 GPa; expected compressive strength 2800 MPa, Poisson's ratio 0.37; parameters of Weibull distribution of tensile strength: scale parameter $\sigma_{cr} = 2500$ MPa and shape parameter $m = 6.1$ and of compressive strength $\sigma_{cr} = 3700$ MPa and $m = 32$ (for X5 fibers) [20].

- **Glass fibers:** radius $r = 17 \mu\text{m}$; expected tensile strength 2500 MPa; Young modulus 72 GPa; expected compressive strength 1500 MPa, Poisson's ratio 0.26; parameters of Weibull distribution of tensile strength: $\sigma_{cr} = 1649$ MPa and $m = 3.09$ [21]. The Weibull parameters of the compressive strength distribution of glass fibers were estimated as follows. The shape parameter $m = 20$ was taken from the experimental studies of compressed pultruded flat sheets [22]. In order to estimate the scale parameter σ_{cr} , we used the following relationship between the average value and the scale parameter:

$$\sigma_{av} = \sigma_{cr} \Gamma(1 + 1/m) \quad (9)$$

Given the estimated average compressive strength of glass fibers 1500 MPa, we can obtain the parameter $\sigma_{cr} = 1500./\Gamma(1.2) = 1500./0.9735 = 1540$ MPa.

- **Epoxy matrix:** Young modulus 3.79 GPa; Poisson's ratio 0.37; and tensile strength 88 MPa [23].

According to the experiments, carried out at the DTU, Risø Campus, no matrix cracks were observed and should be taken into account in these simulations. The interface strengths and misalignment distributions are the same for both types of fibers.

The critical interface stress at which the debonding starts was observed at the level of 25 MPa.

3. Effect of fiber distribution and properties, grouping and clustering

In this section, we consider the combined effect of fiber clustering and the fiber mixing on the damage resistance of composites under axial static loading, tension or compression.

3.1. Effect of mixing fibers; Static loading

Here, we compare the damage resistance of composites under static loading for several cases: homogeneous random fiber distribution with varied fraction of carbon fibers, clustered fiber distribution with “segregated” fiber arrangement (each type of fibers—carbon and glass – have their own clusters) and mixed fiber arrangements (carbon and glass are mixed in the same clusters), with various distributions (carbon fibers localized inside the clusters while glass fibers form the borders of each cluster, and vice versa).

Fig. 2 shows the critical stresses (at which the Young modulus of composite is reduced by 50%) as a function of the fraction of carbon fibers, for tension and compression. The fibers are arranged randomly, the volume content of fibers is set at 18% (calculated as a basic volume content for a unit cell with 200 glass fibers). One can see that the strength of composite under uniform displacement loading decreases when the fibers are mixed, reaches lowest point at the fraction of carbon fibers 40...50% (of all fibers)

and then begins to grow sharply, to achieve the highest point for pure carbon composite. There is a clear and strong difference between hybrid composites with glass and carbon fibers and pure glass or carbon composites: fiber mixing leads always to the reduction the damage resistance under uniform displacement loading. The effect of fiber mixing is different under uniform force loading: in this case, the strength of composite increases with increasing the content of carbon fibers, yet, this effect can be seen clearly only at rather high fraction of carbon fibers.

The negative effect of the fiber mixing on the critical stress of hybrid composites can be explained as follows. Under the axial uniform displacement loading, the stiff, strong fibers bear much larger load than other fibers (s. Eq (2)). If they still fail, the load is redistributed over remaining intact fibers, not equally, but mainly over the fibers close to the failed fiber (see Fig. 4). Thus, the remaining intact fibers, often weaker ones (glass) bear even higher load after the elimination of strong, bearing main load fibers, than in the case of pure glass composite. That leads to the situation when they fail even more intensively in this case. This can be seen in Fig. 5b, right. Here, we can see only failed strong carbon fibers in some clusters, or both failed carbon and glass fibers.

Under compression, adding carbon fibers leads to reduction of the compressive strength of the composite for uniform force loading, and (up to 60% content of carbon) for uniform displacement compressive loading. As expected, the tensile strength is highest for the pure carbon, while the compressive stress is highest for pure glass composites.

The critical stress–carbon fraction curves show competing effects, between the higher stiffness of the composite (due to the in-

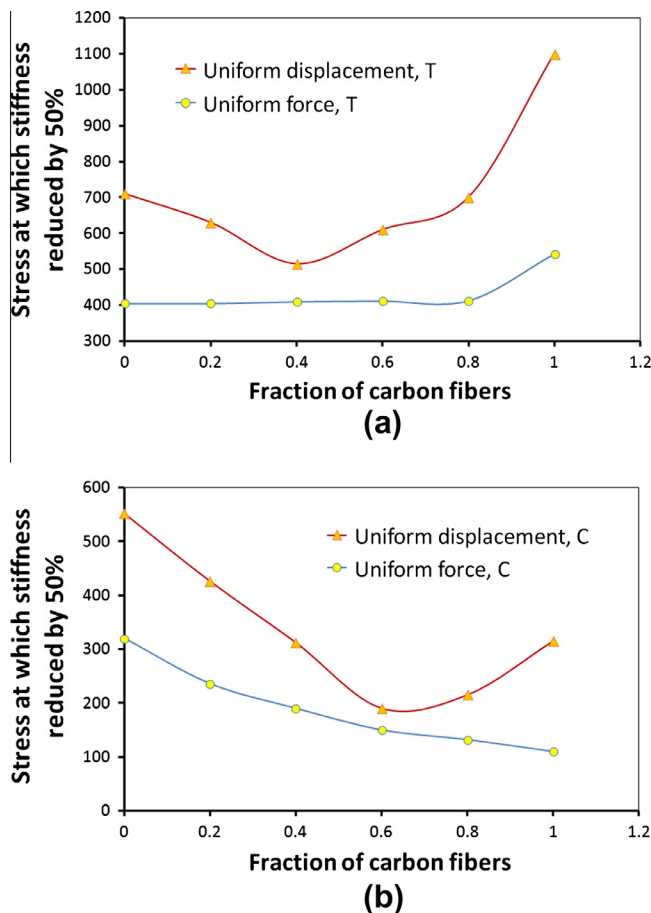


Fig. 2. Critical stress (corresponding to $D = 50\%$) plotted versus the fraction of carbon fibers in hybrid: (a) tension, and (b) compression.

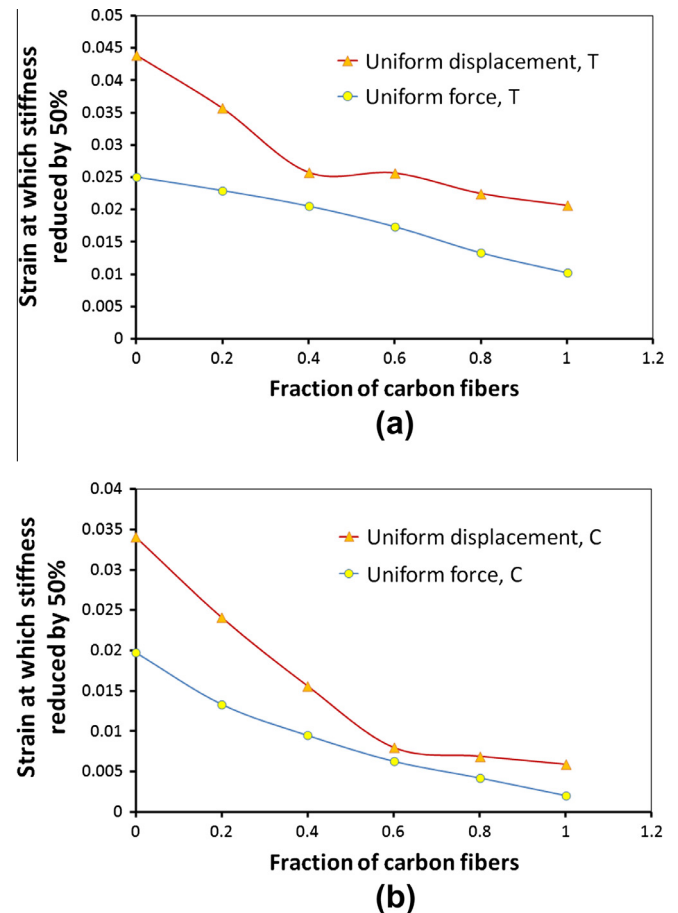


Fig. 3. Critical strain (corresponding to $D = 50\%$) plotted versus the fraction of carbon fibers in hybrid: (a) tension, and (b) compression.

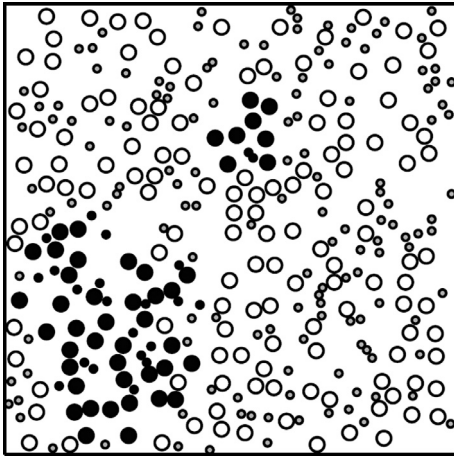


Fig. 4. Uniform force tensile loading: glass fibers fail first then the carbon fibers between “clusters of failed glass fibers”.

crease of carbon fraction) and apparently lower deformability of carbon fibers. This effect can be seen more clearly on the critical strain versus carbon content curves shown in Fig. 3. Here, the critical strain clearly decreases with increasing the fraction of carbon fibers.

As expected, this decrease is especially clearly seen under compression: while under tension, the critical strain of pure glass composite is 2...2.4 times higher than that of pure carbon composite, the critical strain of pure glass composite under compression is 5.7 times (under uniform strain) and even 10 times (under uniform stress) higher than that of pure carbon composite.

3.2. Clustered fiber arrangement: “segregated” versus mixed

In this section, we seek to compare different types of clustered fiber arrangements, in particular, “segregated” (i.e., when different fibers are collected in different clusters) and mixed clusters. A number of unit cells were generated and tested in the model.

Fig. 5 shows damage versus applied stress curves and the distribution of damaged fibers at $D = 0.5$ for tensile loadings of hybrid composites, with random and clustered fiber arrangements. Here, “damage” is defined as the relative reduction of the elastic properties of the material, and calculated as:

$$D = \frac{E_{\text{post-loading}}}{E_{\text{intact-material}}}$$

where E is the Young modulus.

On Fig. 5, we can see again the clear difference for the uniform displacement and uniform force loadings. For the uniform force loading, the segregated clustered structures ensure the lowest damage growth rate and highest strength, even higher than that of random microstructures. For the uniform displacement loading, the damage evolution in segregated microstructures goes more intensively at low loadings than in other structures, yet, again, at the higher loads, the strength of segregated structures is better than that of other structures.

While the “segregated” structures show much slower damage growth rate under uniform force, than under uniform displacement loading, in both cases they ensure the strength of composite higher than other clustered structures (by a few percents for strain controlled, and by 8–14% for uniform displacement cases).

Fig. 5c and d give the distributions of failed fibers for uniform displacement (c) and uniform force (d) loadings, both tension.

As can be seen on Fig. 5c, the failure of fibers is localized at early stages of damage evolution inside each cluster, and that leads to earlier start of damage growth (under the uniform displacement loading of the “segregated” microstructures). In “mixed” structures, fibers in different clusters fail. For the uniform force loading, the clusters of glass fibers fail much more intensively than the clusters of carbon fibers.

For the given material parameters, no kinking of carbon fibers was observed. All the carbon fibers (under compression) failed due to cracking. Apparently, the kinking takes place only for a weaker matrix or as a result of matrix damage.

Let us estimate at which damage degree in the matrix the failure mechanism in the carbon fiber/epoxy system changes from the Weibull-controlled fiber cracking to the kinking (under compression). Estimating the average compressive strength of carbon fibers with the formula (9), we see that the kinking becomes the main mechanisms (at the given properties) if the shear modulus in matrix is strongly damaged, and reduced by 3...4 times.

Further, we investigated the effect of the degree of localization of fibers (in clustered structures) on the damage resistance of the composite. Fig. 6 shows the kinking damage in a unit cell (under the stress 1766 MPa) plotted versus the degree of the localization of fibers, i.e. the amount of fibers in a cluster. It can be seen that the larger distances between the clusters (i.e., higher fiber localization) increase the damage resistance of the composite, apparently, by preventing the “kinking infection” (i.e., when load is redistributed to neighboring fibers after one fiber failure, causing the neighboring fiber failure).

3.3. Effect of load sharing coefficient

Here, we analyze the effect of the load sharing rule on the damage evolution in composites. The stress concentration factor may vary as a result of interface debonding, other nanoscale effects, depends on matrix and interface properties. Let us consider the effect of the power coefficient in the load sharing equation on the damage evolution. We varied the power coefficient in the load sharing equation from 0 (corresponds to global load sharing) to 25 (local load sharing).

Fig. 7 gives the critical stress (at the 50% damage, or 50% stiffness reduction of the composite) plotted versus the power coefficient for pure glass, pure carbon and 50/50 hybrid composite, random fiber arrangement. The volume content of fibers was kept at the level of 18%.

One can see from Fig. 7 that the strength increases with the localization of load redistribution (i.e., with increasing the power coefficient in the load sharing rule (6)). The increase is rather quick when the power coefficient goes from 0 to –5 (i.e., from purely global load sharing to localized load sharing), but remains constant or almost constant in the range of power coefficients from –5 to –20.

It is of interest that the strength of composite increases drastically due to the variation of the load sharing power coefficient by 29...78%. This effect is especially strong for the mixed, 50/50 hybrid composites: the strength of the 50/50 composite increases by 36% and 78% in the cases of stress and uniform displacement loading respectively, when changing the power coefficient from 0 to –10. For the pure composites, the increase is (for carbon) 33% and 29%, and (for glass) 55% and 29% (for stress and uniform displacement loading respectively).

With view on all these conclusions, let us study the possible effect of “wrapping” fiber clusters, i.e. localization of load redistribution after fibers failure inside a cluster. In the “wrapped” bundle (see Fig. 8), the load after a fiber kinks is not redistributed to fibers in other clusters as long as there remain intact fibers in the “home” cluster. Fibers belonging to other bundles do not feel that the fiber

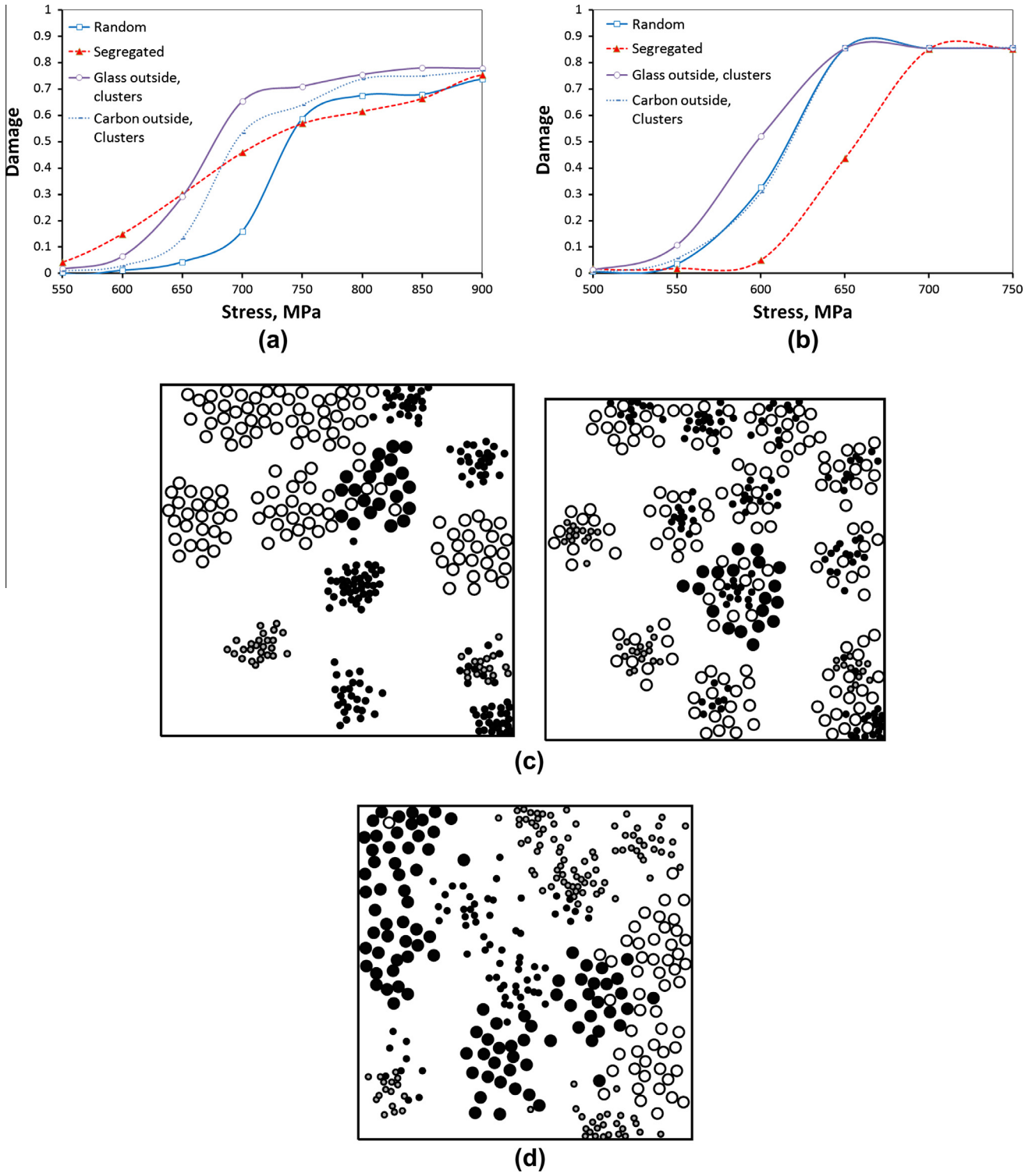


Fig. 5. Damage versus applied stress curves (a and b – strain and stress controlled, tension) and the distribution of damaged fibers at $D = 0.5$ (c, and d, top view) for the loadings of hybrid composites, with clustered fiber arrangements: “segregated”, and mixed. The volume content of all the fibers is set at 20%.

kinked. Only when all the fibers in a cluster fail, the load is redistributed to other clusters.

Fig. 9 shows the compressive damage versus applied stress curves for the “wrapped” and “non-wrapped” clustered structures. The simulations were carried out for pure carbon fibers composite under compressive loading. One can see that the compressive strength of the composite increases by 17%, due to the bundle

wrapping. This corresponds also to the results of the previous section, in which we observed that the localized (inside the clusters) damage growth (in “segregated” clusters) leads to the higher damage resistance of the composite.

Summarizing, one can state that the strength of composites increases with localizing the load distribution after the fiber failure. This effect is more pronounced in non-clustered composites, be-

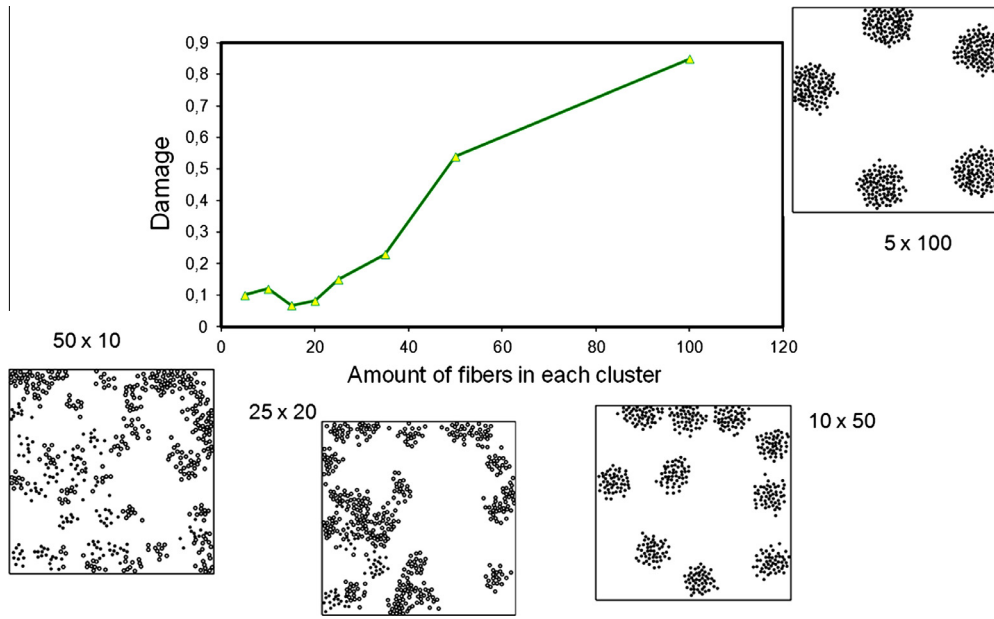


Fig. 6. Effect of the degree of fiber clustering on the kinking damage.

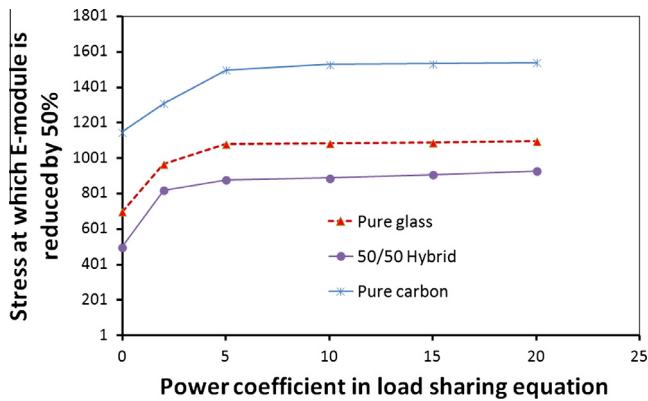


Fig. 7. Effect of load sharing coefficient on the damage evolution (tension) for pure glass, pure carbon and 50/50 hybrid. Strain-controlled loading.

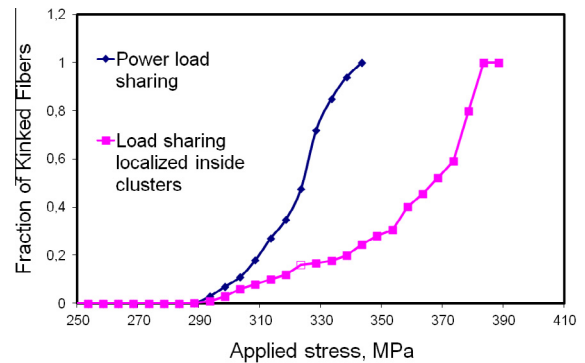


Fig. 9. Comparison of "wrapped" and "non-wrapped" bundles of fibers: Compressive damage versus applied stress curves.

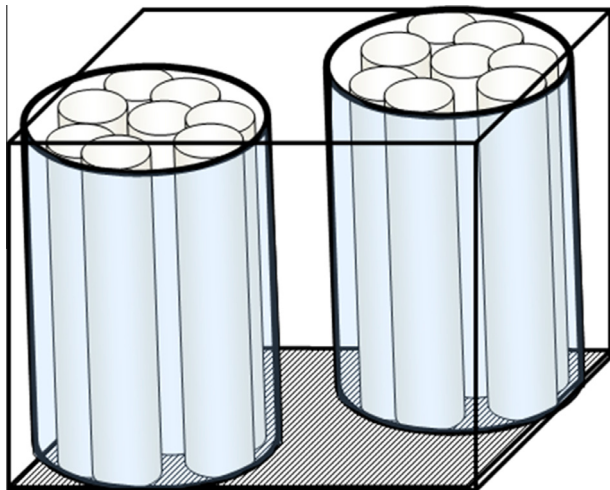


Fig. 8. Schema: "wrapping of fiber bundles": load is shared only inside clusters, not between fibers in different clusters.

cause the clustering itself represents a kind of localizing the load redistribution. The "wrapping", load localization in composites, allows increasing the composite strength.

3.4. Matrix stiffness and nanoreinforcement effects

As demonstrated in [19, see also 24], the additions of even small amount of nanoparticles in the polymer (epoxy) matrix can ensure sufficient increase in the stiffness and elastic parameters of the composite: up to 1.7 times at 0.04 wt% of nanoclay.

So, the question arises on whether this effect can be used to influence the damage resistance of hybrid composites.

First, let us estimate the effect of stiffened versus damaged (weakened) matrix on the fiber failure in composite. We varied the Young modulus of matrix from 0.25 of the standard epoxy value (as given in Section 2) to the 2.5 of that, and simulated the damage growth in the unit cells.

Fig. 10 shows the relative strength of the composite plotted versus the ratio of the Young modulus of the matrix to that of intact epoxy (i.e., from 0.25 to 2.5) (for random fiber arrangement, and uniform displacement tensile loading).

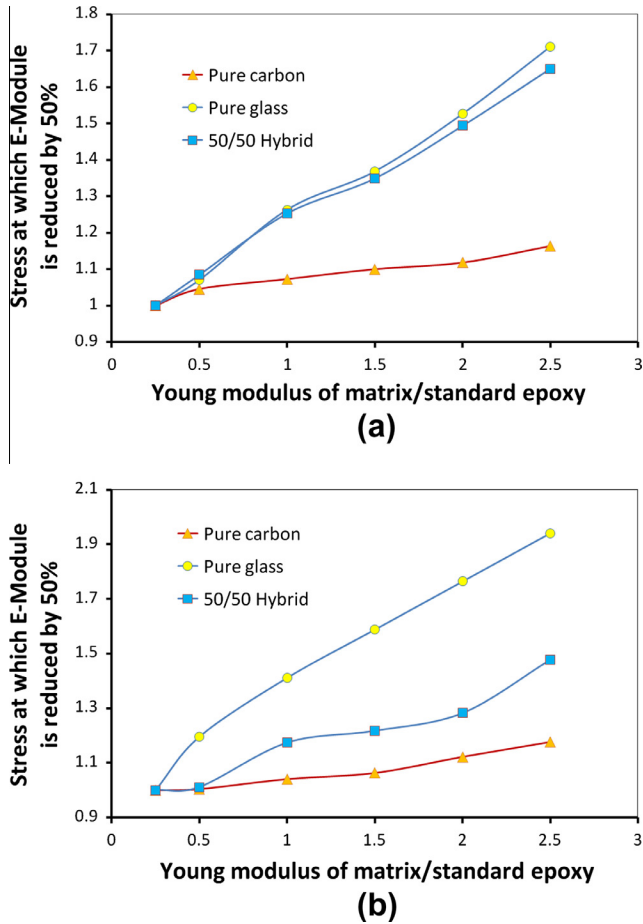


Fig. 10. Matrix effect: Stress of $D = 50\%$ (normalized value) versus Young modulus of the matrix divided by that of standard epoxy, for tension (a) and compression (b) under strain controlled loading.

The strength was calculated as stress at which the stiffness is reduced by 50%, and was normalized over the lowest values (corresponding to the matrix stiffness 0.25 of epoxy), to make the tendencies comparable.

It is of interest that the composites subject to the uniform force loading show very weak dependency of the strength on matrix properties: the difference of strengths of composites with damaged, usual and strengthened matrices (Young modulus 0.25, 1, and 2.5 of that of epoxy) are of the order of 3...4% both for carbon, glass and hybrid reinforced composites.

One can see that the pure glass reinforced and hybrid composites are much more sensitive to the stiffness and damage of matrix than the strong carbon fibers, both for tension and for compression. The apparent conclusion is that the glass reinforced and hybrid composites require much more stiff and damage resistant matrices than the carbon fiber reinforced composites.

The curves for clustered fiber arrangement look very similar to these on Fig. 10, and most parameters are of the same order.

Let us investigate the effect of the nanoclay content of the damage in the composites. Assuming that the nanoclay platelets with aspect ratio 100 and the linear size 100 nm are arranged in clusters, 5 platelets each, the ratio of the Young modulus increase as a function of nanoclay weight content can be approximated by the following equation:

$$E/E_m = 379.97 v_{c_n}^2 + 0.8899 v_{c_n} + 1.0279 \quad (10)$$

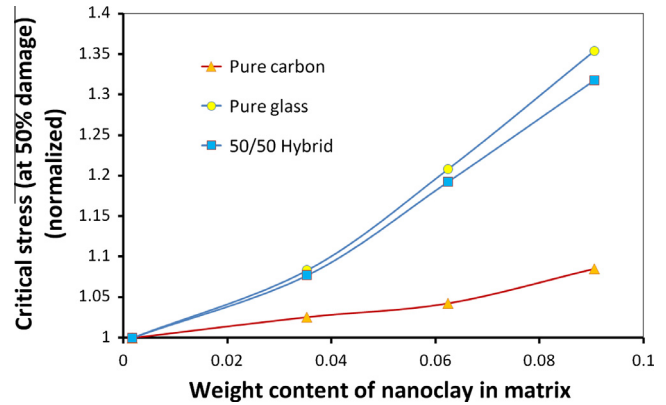


Fig. 11. Effect of nanoreinforcement of the strength of composites.

where vc_n – weight content of nanoclay, E_m – Young modulus of pure epoxy (see Fig. 8 from [19], the curve for $m = 5$ and $z = 0$).

Introducing this relationship into the code “HybridFib”, we can analyze the effect of the nanoreinforcement on the damage of composites. From the simulations (see the curves for tension in Fig. 11), one could see that adding 3.5 wt% of nanoclay particles (100×1 nm) leads to the 7...8% increase in the strength of the composite for mixed and pure glass composite, and small (2...3%) increase in the strength of pure carbon composite. Adding 9 wt% nanoclay leads to the 31...35% strength increase in hybrid and glass composites, and 8% increase in carbon composite (see Fig. 11).

Summarizing the results of this section, we can state the hybrid and glass fiber composites are rather sensitive to the matrix stiffness and damageability. The least sensitive are the pure carbon fiber reinforced composites. Thus, the special attention should be paid to ensure that the matrix for glass reinforced or hybrid composites should be stiff and damage resistant, what can be achieved with the use of the nanoreinforcement.

4. Comparison with 3D finite element computational model and literature data

In Section 3, it was demonstrated that while the replacement of glass fibers by carbon fibers leads to the proportional increase in the stiffness of the composites, it does not necessarily lead to the increase of strength. In fact, the effect of fiber mixing might be different: under uniform displacement tensile loading, the hybrid composites show lower critical stress than the pure carbon or even pure glass composites.

In this section, we seek to verify the results obtained from the developed fiber bundle model by a more exact continuum mechanics model solved by 3D finite element method.

4.1. Generation of multifiber unit cell finite element models for hybrid composites

For the numerical testing of a number of microstructures with varied content of carbon and automatic generation of 3D models of hybrid fiber-reinforced composites, a Python based software code has been developed [29,30]. This program allows also to vary the fiber distribution, e.g. as clustering of fibers and orientation (aligned or unaligned) before generating the fiber-reinforced composites models. The program is described in more details elsewhere [29,30]. The parameters of composites and properties of phases was the same as in Section 2.

The volume content of fibers was taken 45%. The model contains 16 carbon fibers for a pure carbon fiber reinforced composite,

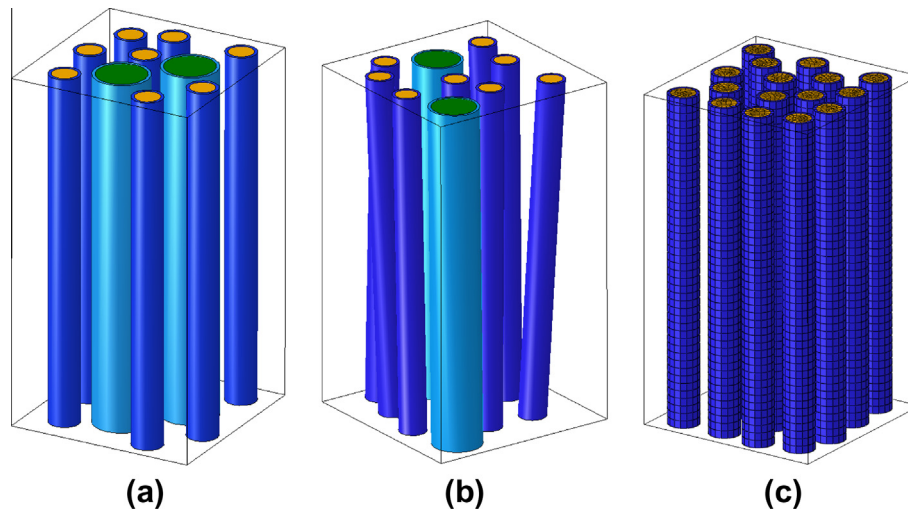


Fig. 12. 3D unit cell models of fiber reinforced composites. (a) Unidirectional. (b) Randomly misaligned. (c) Pure carbon.

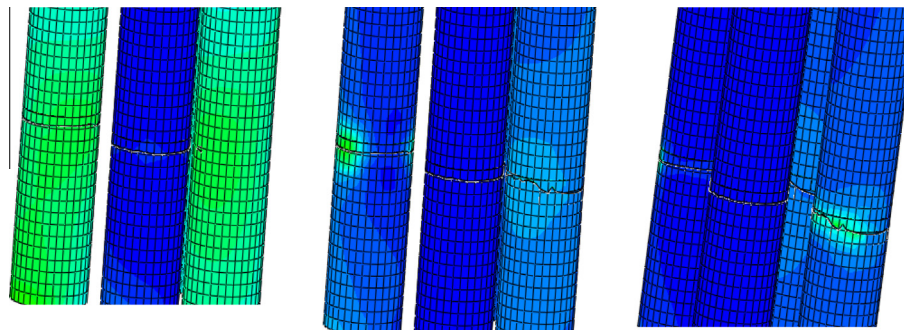


Fig. 13. Crack evolution in glass fibers.

and only 4 fibers when the model was developed for pure glass fiber case. (In other words, volume of one glass fiber equals 4 carbon fibers.)

The 3D hybrid models were subjected to uniaxial displacement loading along the vertical direction.

The crack initiation criterion used in this paper is the maximum principal stress criterion while the criterion for crack propagation analysis is the 3D power law, detailed descriptions of these criteria can be found in authors' previous work [29].

Fig. 12 shows examples of several unit cells. The simulations were carried out using the commercial FE code ABAQUS/STANDARD (version 6.11). 3D finite element 8-node linear brick, reduced integration element C3D8R and three-dimensional 4-node linear tetrahedron element C3D4 were used in the FE analysis.

In order to simulate the crack evolution in hybrid fiber reinforced composites, the linear elastic fracture mechanics (LEFM) approach in conjunction with the framework of the extended-FEM method [31–33] were employed during the damage analysis. The virtual crack closure technique (VCCT) [34,35] is used here to calculate the strain energy release rates.

The material properties are: matrix: $E = 1.9$ GPa, $\nu = 0.37$, tensile strength of 88 MPa, $G_I = 0.103$, $G_{II} = 0.648$, $G_{III} = 0.850$ kJ/m² and carbon fibers: $E = 276$ GPa, $\nu = 0.37$, tensile strength 3000 MPa, $G_I = 3.169$, $G_{II} = 12.183$, $G_{III} = 16.161$ kJ/m². Glass: $E = 72$ GPa, $\nu = 0.26$, tensile strength 2500 MPa, $G_I = 0.682$, $G_{II} = 2.245$, $G_{III} = 2.923$ kJ/m².

4.2. Computational simulations

A series of simulations was carried out. Unit cells with 0%, 25%, 50%, 75% and 100% (volume fraction) of carbon fibers were generated and tested in numerical simulations (under tensile uniform force loading). Fig. 13 shows the simulated crack evolution in glass fibers. The stress strain curves were determined for all the unit cells.

Fig. 14 shows the stress–strain curves for the simulated unit cells. Fig. 15 shows the peak stress and critical material elongation as a function of the fraction of carbon fibers in the composite.

The critical stress slightly increases with increasing the fraction of carbon fibers: it can be observed both in the results obtained from 3D FE model and in the fiber bundle model. As can be seen in Fig. 2a, the critical stress increases by about 28% if all the glass fibers are replaced by the corresponding volume of carbon fibers. In the 3D FE model, the increase is 36%.

The critical elongation of the materials decreases with increasing the fraction of carbon fibers, as can be seen both in the simple fiber bundle and complex 3D micromechanical models are very similar. Comparing the pure carbon and pure glass fiber composites, we can see from Fig. 3a (fiber bundle model) that the critical elongation for pure glass is 72% higher than for pure carbon. For the curves obtained from FE model (Fig. 15), the critical elongation for pure glass fiber composite is 112% higher than for pure carbon. The estimations are not the same (due to apparently different approaches, input data and assumptions), but still they show the sim-

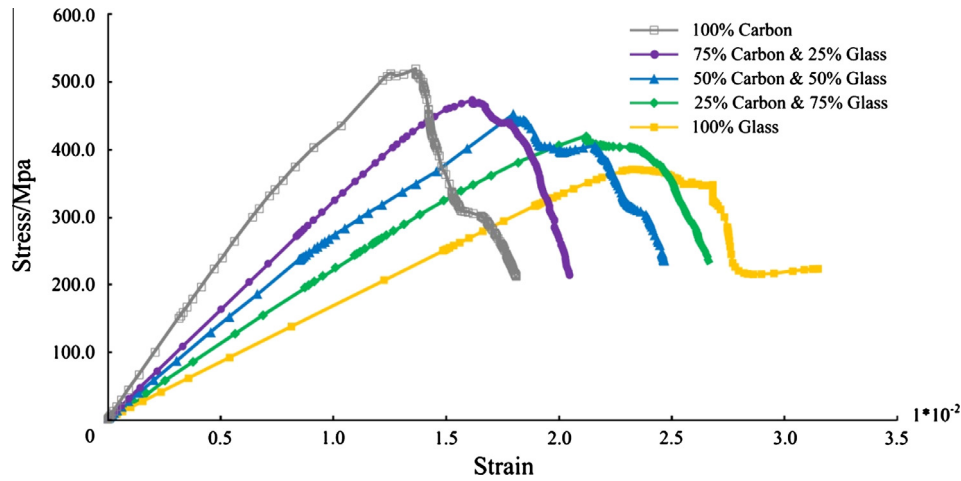


Fig. 14. Stress–strain curves for the simulated unit cells.

ilar qualitative trends: the strong decrease of the critical elongation with increasing the fraction of carbon fibers.

Thus, the exact 3D finite element calculations confirm our conclusions obtained on the basis of the simple fiber bundle model.

4.3. Comparison with literature data

Let us compare our conclusions with some literature data. Bach [25] observed that an increase in fatigue performance of hybrid composites as compared with glass laminates does not fit expectations, especially for $R = -1$ cyclic loading.

Liaw and Delale [26] concluded that glass fiber reinforced composites (in this case, S2 glass) provide the best impact resistance when compared with various hybrid composites. Meanwhile, as Summerscales and Short [6] and Dukes and Griffiths [27] wrote in their paper “there is no change in the stress level at ultimate failure [of hybrid composites] relative to a glass-only composite” under tensile loading (what corresponds to our results, see Fig. 2a). Further, according to [6], “in tension, ... the elongation at first failure is found to be greater than that for the carbon fiber-only composite” (again, as observed in our simulations, see Fig. 3a).

Manders and Bader [28] concluded that “an enhancement of the failure strain of the carbon fiber reinforced phase is observed” when “carbon fiber is combined with less-stiff higher-elongation glass fiber in a hybrid composite”. This is also a conclusion from

our simulations (Fig. 3) where we can see that adding glass fibers to carbon composites increases its failure strain.

Thus, the literature data confirm our main conclusion, namely, that adding strong and expensive carbon fibers into the glass fiber composites does not lead to the positive effects always and automatically. While the stiffness and stress controlled (i.e., uniform force) damage and fatigue behavior are enhanced by replacing weak fibers by strong ones, the strength and failure elongation might be even reduced.

5. Conclusions

In this paper, a fiber bundle based model of damage evolution in hybrid carbon/glass composites has been developed. Using this model, we demonstrated that the hybrid carbon/glass composites (while demonstrating higher stiffness than pure glass composites), can show lower strength and elongation to failure as compared with usual glass fiber polymer composites. The strength (critical stress) of hybrid composites can be lower than that for both pure glass and pure carbon composites, especially under uniform displacement loading. The critical elongation of the hybrid composites decreases with increasing the fraction of carbon fibers in the hybrid. The results obtained from the simplified fiber bundle model were validated by comparison with the 3D finite element model simulations and with the literature data.

Acknowledgements

The author gratefully acknowledges the financial support of the Danish Council for Strategic Research (DSF) via the Sino-Danish collaborative project “High reliability of large wind turbines via computational micromechanics based enhancement of materials performances” (Ref. No. 10-094539) and the Commission of the European Communities through the 7th Framework Programme Grant VINAT (Contract No. 295322). Furthermore, the author is grateful to the DSF for its support via the Danish Centre for Composite Structures and Materials for Wind Turbines (DCCSM) (Contract No. 09-067212).

References

- [1] D.A. Griffin, T.D. Ashwill, *J. Sol. Energy Eng.* 125 (2003) 515.
- [2] C.-H. Ong, S.W. Tsai, The use of carbon fibers in wind turbine blade design: a SERI-8 blade example SAND2000-0478, Sandia National Laboratories Contractor Report, 2000.

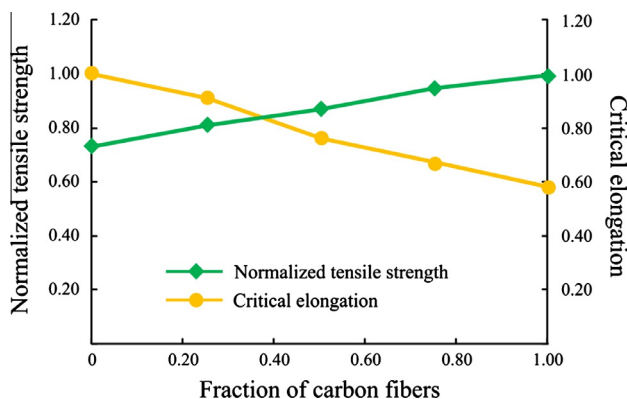


Fig. 15. Normalized critical stress and critical material elongation as a function of the fraction of carbon fibers in the composite.

- [3] M.Y.M. Chiang, X.F. Wang, C.R. Schultheisz, J.M. He, *Compos. Sci. Technol.* 65 (11–12) (2005) 1719–1727.
- [4] J. Gutans, V. Tamuzs, *Theoret. Appl. Fract. Mech.* 7 (3) (June 1987) 193–200.
- [5] L.N. Yao, T.W. Chou, *Compos. Struct.* 12 (1) (1989) 27–37.
- [6] J. Summerscales, D. Short, *Composites* 9 (3) (1978) 157–166.
- [7] P.W. Sonparote, S.C. Lakkad, *Fibre Sci. Technol.* 16 (4) (June 1982) 309–312.
- [8] L. Mishnaevsky Jr., P. Brøndsted, *Comput. Mater. Sci.* 44 (2009) 1351–1359.
- [9] L. Mishnaevsky Jr., P. Brøndsted, *Compos. Sci. Technol.* 69 (3–4) (2009) 477–484.
- [10] L. Mishnaevsky Jr., P. Brøndsted, *Compos. Sci. Technol.* 69 (7–8) (2009) 1036–1044.
- [11] L. Mishnaevsky Jr., P. Brøndsted, *Mater. Sci. Eng., A* 498 (2008) 81–86.
- [12] H. Qing, L. Mishnaevsky Jr., *Comput. Mater. Sci.* 47 (2009) 548–555.
- [13] L. Mishnaevsky Jr., *Compos. Sci. Technol.* 66 (2006) 1873–1887.
- [14] L. Mishnaevsky Jr., N. Lippmann, S. Schmauder, *Int. J. Fract.* 120 (2003) 581–600.
- [15] V.I. Kushch, S.V. Shmegera, L. Mishnaevsky Jr., *Int. J. Solids Struct.* 45 (2008) 2758–2784.
- [16] V.I. Kushch, I. Sevostianov, L. Mishnaevsky Jr., *Int. J. Solids Struct.* 46 (6) (2009) 1574–1588.
- [17] L. Mishnaevsky Jr., *Compos. Sci. Technol.* 71 (2011) 450–460.
- [18] H.D. Wagner, *Compos. Sci. Technol.* 46 (4) (1993) 353–362.
- [19] L. Mishnaevsky Jr., *Compos. Sci. Technol.* 72 (2012) 1167–1177.
- [20] M. Nakatani, M. Shioya, J. Yamashita, *Carbon* 37 (4) (1999) 601–608.
- [21] S. Feih, A. Thrasher, H. Lilholt, *J. Mater. Sci.* 40 (2005) 1615–1623.
- [22] M. Saha et al., *Mech. Compos. Mater.* 36 (6) (2000).
- [23] G. Li, J.E. Helms, S. Pang, K. Schulz, *Polym. Compos.* 22 (5) (2001) 593–603.
- [24] H.W. Wang, H.W. Zhou, R.D. Peng, L. Mishnaevsky Jr., *Compos. Sci. Technol.* 71 (7) (2011) 980–988.
- [25] P.W. Bach, *Fatigue properties of glass- and glass/carbon-polyester composites for wind turbines*, Energy research Centre of the Netherlands report: ECN-C-92-072, Petten, the Netherlands, 1992.
- [26] B. Liaw, F. Delale, *Hybrid carbon-glass fiber/toughened epoxy thick composite joints subject to drop-weight and ballistic impacts*, final report, US Army Research Office, 2007.
- [27] R. Dukes, D.L. Griffiths, *Marine aspects of carbon fibre and glass fibre/carbon fibre composites*, in: 1st International Conference on Carbon Fibres, paper 28, The Plastics Institute, London, 1971. pp. 226–231.
- [28] P.W. Manders, M.G. Bader, *J. Mater. Sci.* 16 (8) (1981) 2246–2256.
- [29] G.M. Dai, *Compos. Sci. Technol.* 74 (2013) 67–77.
- [30] G.M. Dai, L. Mishnaevsky Jr., *Fatigue of hybrid glass/carbon composites: computational studies*, (in preparation).
- [31] T. Belytschko, R. Gracie, G. Ventura, *Modell. Simul. Mater. Sci. Eng.* 17 (2009) 1–24.
- [32] M. Stolarska, D.L. Chopp, N. Moes, T. Belytschko, *Int. J. Numer. Meth. Eng.* 51 (2001) 943–960.
- [33] N. Sukumar, N. Moes, B. Moran, T. Belytschko, *Int. J. Numer. Meth. Eng.* 48 (2000) 1549–1570.
- [34] E.F. Rybicki, M.F. Kanninen, *Eng. Fract. Mech.* 9 (1977) 931–938.
- [35] R. Krueger, *Appl. Mech. Rev.* 57 (2004) 109–143.